

Discovery of the VHE gamma-ray source HESS J1832-093 in the vicinity of SNR G22.7-0.2

A. Abramowski, Fabio Acero, F. Aharonian, F. Ait Benkhali, A. G. Akhperjanian, E. Angüner, G. Anton, S. Balenderan, Agnès Balzer, A. Barnacka, et al.

▶ **To cite this version:**

A. Abramowski, Fabio Acero, F. Aharonian, F. Ait Benkhali, A. G. Akhperjanian, et al.. Discovery of the VHE gamma-ray source HESS J1832-093 in the vicinity of SNR G22.7-0.2. Monthly Notices of the Royal Astronomical Society, 2015, 446, pp.1163-1169. 10.1093/mnras/stu2148 . in2p3-01085027

HAL Id: in2p3-01085027
https://hal.in2p3.fr/in2p3-01085027

Submitted on 23 Jun 2021

HAL is a multi-disciplinary open access archive for the deposit and dissemination of scientific research documents, whether they are published or not. The documents may come from teaching and research institutions in France or abroad, or from public or private research centers.

L'archive ouverte pluridisciplinaire **HAL**, est destinée au dépôt et à la diffusion de documents scientifiques de niveau recherche, publiés ou non, émanant des établissements d'enseignement et de recherche français ou étrangers, des laboratoires publics ou privés.



Distributed under a Creative Commons Attribution 4.0 International License

arXiv:1411.0572v1 [astro-ph.HE] 3 Nov 2014

Discovery of the VHE gamma-ray source HESS J1832−093 in the vicinity of SNR G22.7−0.2

H.E.S.S. Collaboration, A. Abramowski,[1] F. Acero,[41,*] F. Aharonian,[2,3,4] F. Ait Benkhali,[2] A.G. Akhperjanian,[5,4] E. Angüner,[6] G. Anton,[7] S. Balenderan,[8] A. Balzer,[9,10] A. Barnacka,[11] Y. Becherini,[12] J. Becker Tjus,[13] K. Bernlöhr,[2,6] E. Birsin,[6] E. Bissaldi,[14] J. Biteau,[15] M. Böttcher,[16] C. Boisson,[17] J. Bolmont,[18] P. Bordas,[19] J. Brucker,[7] F. Brun,[2] P. Brun,[20] T. Bulik,[21] S. Carrigan,[2] S. Casanova,[16,2] M. Cerruti,[17,22] P.M. Chadwick,[8] R. Chalme-Calvet,[18] R.C.G. Chaves,[20] A. Cheesebrough,[8] M. Chrétien,[18] A.-C. Clapson,[42] S. Colafrancesco,[23] G. Cologna,[24] J. Conrad,[25,26] C. Couturier,[18] Y. Cui,[19] M. Dalton,[27,28] M.K. Daniel,[8] I.D. Davids,[16,29] B. Degrange,[15] C. Deil,[2] P. deWilt,[30] H.J. Dickinson,[25] A. Djannati-Ataï,[31] W. Domainko,[2] L.O'C. Drury,[3] G. Dubus,[32] K. Dutson,[33] J. Dyks,[11] M. Dyrda,[34] T. Edwards,[2] K. Egberts,[14] P. Eger,[2] P. Espigat,[31] C. Farnier,[25] S. Fegan,[15] F. Feinstein,[35] M.V. Fernandes,[1] D. Fernandez,[35] A. Fiasson,[36] G. Fontaine,[15] A. Förster,[2] M. Füßling,[10] M. Gajdus,[6] Y.A. Gallant,[35] T. Garrigoux,[18] G. Giavitto,[9] B. Giebels,[15] J.F. Glicenstein,[20] M.-H. Grondin,[2,24] M. Grudzińska,[21] S. Häffner,[7] J. Hahn,[2] J. Harris,[8] G. Heinzelmann,[1] G. Henri,[32] G. Hermann,[2] O. Hervet,[17] A. Hillert,[2] J.A. Hinton,[33] W. Hofmann,[2] P. Hofverberg,[2] M. Holler,[10] D. Horns,[1] A. Jacholkowska,[18] C. Jahn,[7] M. Jamrozy,[37] M. Janiak,[11] F. Jankowsky,[24] I. Jung,[7] M.A. Kastendieck,[1] K. Katarzyński,[38] U. Katz,[7] S. Kaufmann,[24] B. Khélifi,[31] M. Kieffer,[18] S. Klepser,[9] D. Klochkov,[19] W. Kluźniak,[11] T. Kneiske,[1] D. Kolitzus,[14] Nu. Komin,[36] K. Kosack,[20] S. Krakau,[13] F. Krayzel,[36] P.P. Krüger,[16,2] H. Laffon,[27,*] G. Lamanna,[36] J. Lefaucheur,[31] A. Lemière,[31] M. Lemoine-Goumard,[27] J.-P. Lenain,[18] D. Lennarz,[2] T. Lohse,[6] A. Lopatin,[7] C.-C. Lu,[2] V. Marandon,[2] A. Marcowith,[35] R. Marx,[2] G. Maurin,[36] N. Maxted,[30] M. Mayer,[10] T.J.L. McComb,[8] J. Méhault,[27,28] P.J. Meintjes,[39] U. Menzler,[13] M. Meyer,[25] R. Moderski,[11] M. Mohamed,[24] E. Moulin,[20] T. Murach,[6] C.L. Naumann,[18] M. de Naurois,[15] J. Niemiec,[34] S.J. Nolan,[8] L. Oakes,[6] S. Ohm,[33] E. de Oña Wilhelmi,[2] B. Opitz,[1] M. Ostrowski,[37] I. Oya,[6] M. Panter,[2] R.D. Parsons,[2] M. Paz Arribas,[6] N.W. Pekeur,[16] G. Pelletier,[32] J. Perez,[14] P.-O. Petrucci,[32] B. Peyaud,[20] S. Pita,[31] H. Poon,[2] G. Pühlhofer,[19] M. Punch,[31] A. Quirrenbach,[24] S. Raab,[7] M. Raue,[1] A. Reimer,[14] O. Reimer,[14] M. Renaud,[35] R. de los Reyes,[2] F. Rieger,[2] L. Rob,[40] C. Romoli,[3] S. Rosier-Lees,[36] G. Rowell,[30] B. Rudak,[11] C.B. Rulten,[17] V. Sahakian,[5,4] D.A. Sanchez,[2,36] A. Santangelo,[19] R. Schlickeiser,[13] F. Schüssler,[20] A. Schulz,[9] U. Schwanke,[6] S. Schwarzburg,[19] S. Schwemmer,[24] H. Sol,[17] G. Spengler,[6] F. Spies,[1] Ł. Stawarz,[37] R. Steenkamp,[29] C. Stegmann,[10,9] F. Stinzing,[7] K. Stycz,[9] I. Sushch,[6,16] A. Szostek,[37] J.-P. Tavernet,[18] T. Tavernier,[31] A.M. Taylor,[3] R. Terrier,[31] M. Tluczykont,[1] C. Trichard,[36] K. Valerius,[7] C. van Eldik,[7] B. van Soelen,[39] G. Vasileiadis,[35] C. Venter,[16] A. Viana,[2] P. Vincent,[18] H.J. Völk,[2] F. Volpe,[2] M. Vorster,[16] T. Vuillaume,[32] S.J. Wagner,[24] P. Wagner,[6] M. Ward,[8] M. Weidinger,[13] Q. Weitzel,[2] R. White,[33] A. Wierzcholska,[37] P. Willmann,[7] A. Wörnlein,[7] D. Wouters,[20] V. Zabalza,[2] M. Zacharias,[13] A. Zajczyk,[11,35] A.A. Zdziarski,[11] A. Zech,[17] H.-S. Zechlin[1]

[1] *Universität Hamburg, Institut für Experimentalphysik, Luruper Chaussee 149, D 22761 Hamburg, Germany*
[2] *Max-Planck-Institut für Kernphysik, P.O. Box 103980, D 69029 Heidelberg, Germany*
[3] *Dublin Institute for Advanced Studies, 31 Fitzwilliam Place, Dublin 2, Ireland*
[4] *National Academy of Sciences of the Republic of Armenia, Yerevan*
[5] *Yerevan Physics Institute, 2 Alikhanian Brothers St., 375036 Yerevan, Armenia*
[6] *Institut für Physik, Humboldt-Universität zu Berlin, Newtonstr. 15, D 12489 Berlin, Germany*
[7] *Universität Erlangen-Nürnberg, Physikalisches Institut, Erwin-Rommel-Str. 1, D 91058 Erlangen, Germany*
[8] *University of Durham, Department of Physics, South Road, Durham DH1 3LE, U.K.*
[9] *DESY, D-15738 Zeuthen, Germany*
[10] *Institut für Physik und Astronomie, Universität Potsdam, Karl-Liebknecht-Strasse 24/25, D 14476 Potsdam, Germany*
[11] *Nicolaus Copernicus Astronomical Center, ul. Bartycka 18, 00-716 Warsaw, Poland*
[12] *Department of Physics and Electrical Engineering, Linnaeus University, 351 95 Växjö, Sweden*
[13] *Institut für Theoretische Physik, Lehrstuhl IV: Weltraum und Astrophysik, Ruhr-Universität Bochum, D 44780 Bochum, Germany*
[14] *Institut für Astro- und Teilchenphysik, Leopold-Franzens-Universität Innsbruck, A-6020 Innsbruck, Austria*
[15] *Laboratoire Leprince-Ringuet, Ecole Polytechnique, CNRS/IN2P3, F-91128 Palaiseau, France*
[16] *Centre for Space Research, North-West University, Potchefstroom 2520, South Africa*
[17] *LUTH, Observatoire de Paris, CNRS, Université Paris Diderot, 5 Place Jules Janssen, 92190 Meudon, France*
[18] *LPNHE, Université Pierre et Marie Curie Paris 6, Université Denis Diderot Paris 7, CNRS/IN2P3, 4 Place Jussieu, F-75252, Paris Cedex 5, France*
[19] *Institut für Astronomie und Astrophysik, Universität Tübingen, Sand 1, D 72076 Tübingen, Germany*
[20] *DSM/Irfu, CEA Saclay, F-91191 Gif-Sur-Yvette Cedex, France*
[21] *Astronomical Observatory, The University of Warsaw, Al. Ujazdowskie 4, 00-478 Warsaw, Poland*
[22] *now at Harvard-Smithsonian Center for Astrophysics, 60 garden Street, Cambridge MA, 02138, USA*
[23] *School of Physics, University of the Witwatersrand, 1 Jan Smuts Avenue, Braamfontein, Johannesburg, 2050 South Africa*
[24] *Landessternwarte, Universität Heidelberg, Königstuhl, D 69117 Heidelberg, Germany*
[25] *Oskar Klein Centre, Department of Physics, Stockholm University, Albanova University Center, SE-10691 Stockholm, Sweden*
[26] *Wallenberg Academy Fellow*
[27] *Université Bordeaux 1, CNRS/IN2P3, Centre d'Études Nucléaires de Bordeaux Gradignan, 33175 Gradignan, France*
[28] *Funded by contract ERC-StG-259391 from the European Community*
[29] *University of Namibia, Department of Physics, Private Bag 13301, Windhoek, Namibia*
[30] *School of Chemistry & Physics, University of Adelaide, Adelaide 5005, Australia*
[31] *APC, AstroParticule et Cosmologie, Université Paris Diderot, CNRS/IN2P3, CEA/Irfu, Observatoire de Paris, Sorbonne Paris Cité, 10, rue Alice Domon et Léonie Duquet, 752*
[32] *UJF-Grenoble 1 / CNRS-INSU, Institut de Planétologie et d'Astrophysique de Grenoble (IPAG) UMR 5274, Grenoble, F-38041, France*
[33] *Department of Physics and Astronomy, The University of Leicester, University Road, Leicester, LE1 7RH, United Kingdom*
[34] *Instytut Fizyki Jądrowej PAN, ul. Radzikowskiego 152, 31-342 Kraków, Poland*
[35] *Laboratoire Univers et Particules de Montpellier, Université Montpellier 2, CNRS/IN2P3, CC 72, Place Eugène Bataillon, F-34095 Montpellier Cedex 5, France*
[36] *Laboratoire d'Annecy-le-Vieux de Physique des Particules, Université de Savoie, CNRS/IN2P3, F-74941 Annecy-le-Vieux, France*
[37] *Obserwatorium Astronomiczne, Uniwersytet Jagielloński, ul. Orla 171, 30-244 Kraków, Poland*
[38] *Toruń Centre for Astronomy, Nicolaus Copernicus University, ul. Gagarina 11, 87-100 Toruń, Poland*
[39] *Department of Physics, University of the Free State, PO Box 339, Bloemfontein 9300, South Africa*
[40] *Charles University, Faculty of Mathematics and Physics, Institute of Particle and Nuclear Physics, V Holešovičkách 2, 180 00 Prague 8, Czech Republic*
[41] *Laboratoire AIM, CEA-IRFU/CNRS/Université Paris Diderot, Service d'Astrophysique, CEA Saclay, 91191 Gif sur Yvette, France*
[42] *European Molecular Biology Laboratory, Meyerhofstrasse 1, 69117 Heidelberg, Germany*

[*] *E-mail: laffon@cenbg.in2p3.fr (Hélène Laffon); fabio.acero@cea.fr (Fabio Acero)*

Mon. Not. R. Astron. Soc. **000**, 2–6 (2014) Printed 19 October 2018 (MN LATEX style file v2.2)

ABSTRACT

The region around the supernova remnant (SNR) W41 contains several TeV sources and has prompted the H.E.S.S. Collaboration to perform deep observations of this field of view. This resulted in the discovery of the new very high energy (VHE) source HESS J1832−093, at the position RA = $18^{h}32^{m}50^{s} \pm 3^{s}_{stat} \pm 2^{s}_{syst}$, Dec = $-9°22'36'' \pm 32''_{stat} \pm 20''_{syst}$ (J2000), spatially coincident with a part of the radio shell of the neighboring remnant G22.7−0.2. The photon spectrum is well described by a power-law of index $\Gamma = 2.6 \pm 0.3_{stat} \pm 0.1_{syst}$ and a normalization at 1 TeV of $\Phi_0 = (4.8 \pm 0.8_{stat} \pm 1.0_{syst}) \times 10^{-13}\,cm^{-2}\,s^{-1}\,TeV^{-1}$. The location of the gamma-ray emission on the edge of the SNR rim first suggested a signature of escaping cosmic-rays illuminating a nearby molecular cloud. Then a dedicated *XMM-Newton* observation led to the discovery of a new X-ray point source spatially coincident with the TeV excess. Two other scenarios were hence proposed to identify the nature of HESS J1832−093. Gamma-rays from inverse Compton radiation in the framework of a pulsar wind nebula scenario or the possibility of gamma-ray production within a binary system are therefore also considered. Deeper multi-wavelength observations will help to shed new light on this intriguing VHE source.

Key words: astroparticle physics - gamma rays: general - ISM: individual objects: HESS J1832−093- ISM: individual objects: SNR G22.7−0.2

1 INTRODUCTION

H.E.S.S. (High Energy Stereoscopic System) is an array of five imaging atmospheric Cherenkov telescopes located 1800 m above sea level in the Khomas Highland of Namibia. The first four telescopes have been fully operational since 2004 (Aharonian et al. 2006a), while the fifth telescope started operation in September 2012. The H.E.S.S. Collaboration has been conducting a systematic scan of the Galactic plane, which led to the discovery of a rich population of very high energy (VHE, E⩾100 GeV) gamma-ray sources. The majority of these galactic sources are extended beyond the H.E.S.S. point spread function (PSF), which is of the order of 6′, and mostly comprise supernova remnants (SNRs) and evolved pulsar wind nebulae (PWNe). Point-like sources are also observed in the Galactic plane and are generally associated with gamma-ray binaries (e.g. LS 5039, Aharonian et al. (2006c)) and with young PWNe such as G0.9+0.1 (Aharonian et al. 2005a). Furthermore, in the particular case of HESS J1943+213, an identification of the VHE point-like source in the Galactic plane with a background active galactic nucleus (AGN) is currently the most likely hypothesis (Abramowski et al. 2011a).

The paper at hand deals with the field of view around SNR G22.7−0.2, which is close to SNR W41 in sky projection. The discovery of a new point-like TeV source, HESS J1832−093, is reported in Section 2 as well as the search for a GeV counterpart with the *Fermi*-LAT. The TeV emission lies close (about 1′ away) to the radio rim of the supernova remnant G22.7−0.2. This SNR shows a non-thermal ring of 26′ diameter in radio (Shaver & Goss 1970) and partially overlaps the neighboring remnant W41. However, there is no obvious flux enhancement in the radio data around the position of HESS J1832−093. Using the Σ-D relation given by Guseinov et al. (2003a) which connects the surface brightness Σ of a supernova remnant with its diameter D, the estimated distance to G22.7−0.2 is approximately (3.7±1.1) kpc (Guseinov et al. 2003b). The source location at the edge of the SNR shell could suggest a signature of escaping hadronic cosmic-rays which would illuminate dense material such as molecular clouds. Such scenario is considered a prime opportunity to unambiguously study hadronic cosmic-rays accelerated in supernova remnants. This possibility is examined in Section 3. However, the compact nature of the TeV emission together with the detection of a new X-ray counterpart is at odds with this scenario. Dedicated *XMM-Newton* data at the position of HESS J1832−093 have led to the discovery of this new potential counterpart, the X-ray point source XMMU J183245−0921539, as detailed in Section 4. As a consequence, two scenarios of compact objects, a young PWN or a binary system origin, are considered in Section 4 in order to explain the VHE emission.

2 MULTI-WAVELENGTH DATA ANALYSIS

2.1 H.E.S.S.

A standard analysis method with Hillas event reconstruction (Aharonian et al. 2006a) is adopted to study the field of view of interest. A multi-variate analysis is used (Becherini et al. 2011) to provide improved discrimination between hadrons and gamma-rays. A minimum charge cut of 110 photo-electrons in the shower images is applied to the data, resulting in an energy threshold of about 450 GeV.

A standard run selection procedure is used to remove bad quality observations in order to study the newly discovered source. The available data set in this region covers a zenith angle ranging between 13° and 50° (mean value of 25°) and comprises 67 hours live time of observations, taken from 2004 to 2011. Using this data set, the new source, named HESS J1832−093, is detected with a peak significance of 7.9 σ pre-trials, corresponding to a post-trial detection significance of 5.6 σ. The average angular resolution (r_{68}) obtained for the selected data set is 0.081° at the source position. The excess map of the field of view centered on the new detected source and smoothed with the r_{68} value is presented in Fig. 1.

A two-dimensional symmetrical Gaussian function is used to determine the position and size of the TeV emission with a χ^2 minimization. The best-fit position is RA = $18^{h}32^{m}50^{s} \pm 3^{s}_{stat} \pm 2^{s}_{syst}$, Dec = $-9°22'36'' \pm 32''_{stat} \pm 20''_{syst}$ (J2000) (χ^2/ndf=0.89). No significant extension was found for the source and an upper limit of 0.074° at a 99% confidence level (C.L.) is derived.

In order to broaden the accessible energy range the charge cut of the shower images is lowered to a minimum of 80 photo-electrons, resulting in an energy threshold of ∼400 GeV. The forward-folding method described in Aharonian et al. (2006a) is applied to the data to derive the spectrum. Source counts are extracted from a circular region of 0.1° radius around the best fit position of HESS J1832−093, a size optimized for point source studies with the applied cuts (Becherini et al. 2011).

The spectrum obtained between 400 GeV and 5 TeV (displayed in Fig. 2) is well described by a power-law (PL) $\frac{d\Phi}{dE} = \Phi_0 \left(\frac{E}{1\,TeV}\right)^{-\Gamma}$, with an index $\Gamma = 2.6 \pm 0.3_{stat} \pm 0.1_{syst}$ and a dif-

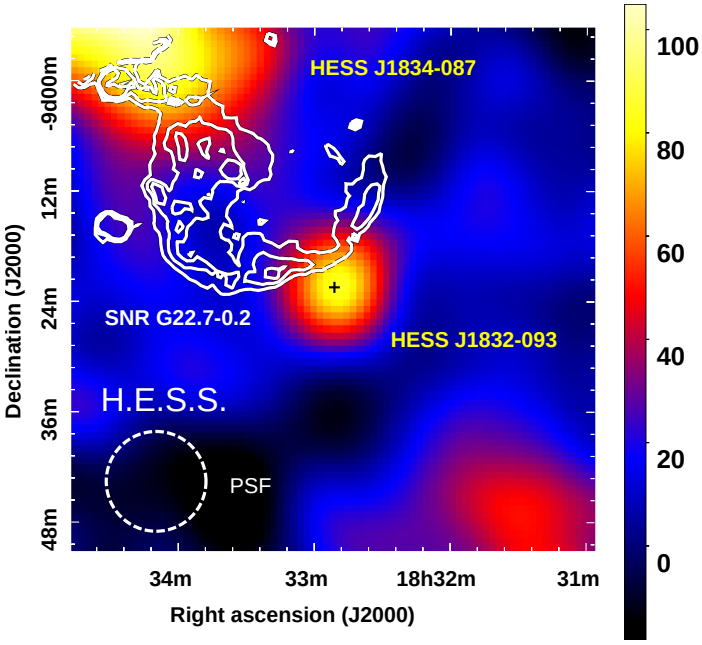


Figure 1. H.E.S.S. excess map smoothed with a 2D-gaussian of width corresponding to the r_{68} value of 0.081° (represented by the dashed circle). Units are counts per integration area. The best-fit position of HESS J1832−093 with statistical errors is represented by the black cross. The SNR G22.7−0.2 observed at 1.4 GHz (Helfand et al. 2006) is represented by the white contours. The emission seen on the upper left is a small part of HESS J1834−087 (Aharonian et al. 2006b), the TeV source in spatial coincidence with SNR W41.

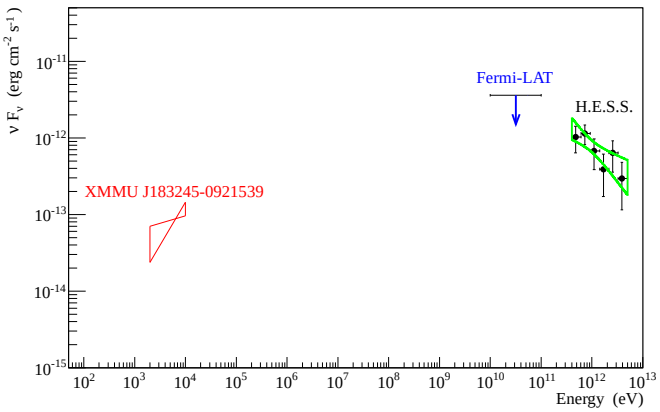


Figure 2. Spectral energy distribution from the region of VHE emission from HESS J1832−093. The VHE gamma-ray spectrum observed with H.E.S.S. is displayed together with the upper limit obtained between 10 and 100 GeV with the Fermi-LAT. The green contour represents the 1 σ confidence level of the fitted spectrum using a power-law hypothesis. Only statistical errors (68% confidence level) are shown for the spectral points. The X-ray power-law model of XMMU J183245−0921539 is overlaid in red, taking into account the statistical uncertainties only.

ferential flux normalization at 1 TeV of $\Phi_0 = (4.8 \pm 0.8_{\rm stat} \pm 1.0_{\rm syst}) \times 10^{-13}\,{\rm cm^{-2}\,s^{-1}\,TeV^{-1}}$. The integrated flux above 1 TeV is $I(E > 1\,{\rm TeV}) = (3.0 \pm 0.8_{\rm stat} \pm 0.6_{\rm syst}) \times 10^{-13}\,{\rm cm^{-2}\,s^{-1}}$, corresponding roughly to 1% of the Crab Nebula flux above the same energy (Aharonian et al. 2006a).

A search for curvature in the gamma-ray spectrum was performed by fitting log-parabola and exponential cutoff power-law models to the data. While not ruled out, these models are not favored since the improvement in fit quality compared to the simple power-law model is not statistically significant.

Long-term light curves were produced with different integrated times (run, night and month) and Z-transformed discrete correlation functions (Alexander 1997) were applied to the data to look for periodicity. However no significant temporal variability was detected in the H.E.S.S. data set.

2.2 *Fermi*-LAT

The Fermi Large Area Telescope (LAT) is a gamma-ray telescope operating in the 20 MeV to 300 GeV energy range (Atwood et al. 2009). No *Fermi*-LAT source is listed at the position of HESS J1832−093 in the Fermi 2-year catalog (2FGL, Nolan et al. 2012). However, this field of view located close to the Galactic plane is very rich in gamma-ray sources and diffuse emission, making the analysis challenging. Furthermore, the *Fermi* source 2FGL J1834.3-0848, in spatial coincidence with SNR W41, lies very close to HESS J1832−093 and the *Fermi* angular resolution at low energy does not allow different potential contributions to this source to be distinguished. Therefore a dedicated analysis was performed in the field of view to look for a potential counterpart in the GeV range. The analysis was carried out with 4 years of data and above 10 GeV as a compromise between statistics and background from the diffuse Galactic emission (dominating for $E < 10$ GeV). The Instrument Response Functions (IRFs) P7SOURCE_V6 and the *Source* class events were used (see Ackermann et al. 2012, for details about the event classification and IRFs). The corresponding Galactic diffuse background (gal_2yearp7v6_v0.fits) and the extragalactic isotropic background (iso_p7v6source.txt), distributed with the Fermi Science Tools[1], were used. In addition to the diffuse backgrounds, a model of the nearby sources within a 5° radius was built based on the 2FGL catalog (Nolan et al. 2012). No significant gamma-ray excess is found on top of the model previously built. An energy flux upper limit of $3.6 \times 10^{-12}\,{\rm erg\,cm^{-2}\,s^{-1}}$ in the 10-100 GeV band is then obtained at 99% C.L., assuming a point source at the position of HESS J1832−093. This upper limit is shown on the spectral energy distribution (SED) displayed on Fig. 2.

2.3 *XMM-Newton*

In order to constrain the nature of the source HESS J1832−093, a dedicated observation with the X-ray *XMM-Newton* satellite was performed in March 2011 for 17 ks. After filtering out proton flare contamination, 13 ks and 7 ks of exposure time remained for the two EPIC-MOS cameras and for the EPIC-pn camera, respectively. The data were processed using the *XMM-Newton* Science Analysis System (v10.0). The instrumental background was derived from a compilation of blank sky observations (Carter & Read 2007), renormalized to the actual exposure using the count rate in the 10-12 keV energy band.

The brightest object in the *XMM-Newton* field of view is a point-like source (Source A in Fig. 3) located at RA = $18^{\rm h}32^{\rm m}45^{\rm s}.04$, Dec = −9° 21′ 53″.9 with a 90% C.L. error radius of 2.3″ which is 1.5′ away from the best-fit position of the H.E.S.S.

[1] http://fermi.gsfc.nasa.gov/ssc/data/analysis/

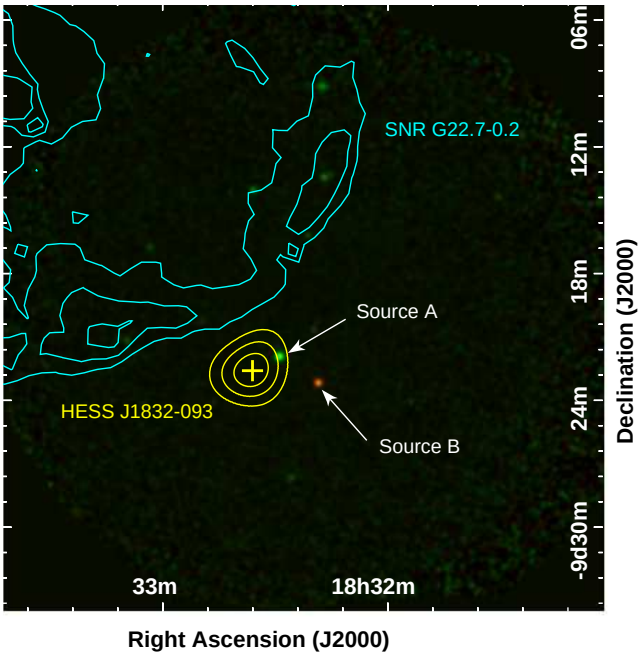


Figure 3. XMM-Newton composite flux map of the field of view around HESS J1832−093 in the 0.5-2 keV (red) and 2-6 keV (green) energy ranges. The SNR G22.7−0.2 observed at 1.4 GHz is overlaid in cyan contours. The yellow cross symbolizes the best-fit position of HESS J1832−093 with corresponding errors. The confidence contour levels (68%, 95% and 99%) of the source position fit are also shown in yellow. Two point-like sources are detected near the position of HESS J1832−093: Sources A and B discussed in Section 2.3. No diffuse emission from the SNR shell segment is seen in the X-ray data. The maximal flux values are 3.5×10^{-4} cm^{-2} s^{-1}arcmin^{-2} and 3.6×10^{-4} cm^{-2} s^{-1}arcmin^{-2} for the red and green maps, respectively.

excess. This new source, named XMMU J183245−0921539, is located within the 99% C.L. contours of the H.E.S.S. best fit position and is a potential counterpart to the VHE source. Other point sources detected in the field of view are either too soft (such as Source B, Fig. 3) or too far away from HESS J1832−093 to be considered as potential counterparts.

Spectra from the three instruments were extracted from a 15′ radius circular region centered on XMMU J183245−0921539. Both an absorbed power-law model and an absorbed black body model were tested. The best fit parameters for the power-law model are a column density $N_H = 10.5^{+3.1}_{-2.7} \times 10^{22}$ cm^{-2}, a photon index $\Gamma = 1.3^{+0.5}_{-0.4}$ and an unabsorbed energy flux Φ(2-10 keV)= $6.9^{+1.7}_{-2.8} \times 10^{-13}$ erg cm^{-2} s^{-1}, with a p-value[2] of 0.75. The absorbed black-body fit yields $N_H = 5.5^{+1.3}_{-1.8} \times 10^{22}$ cm^{-2}, a temperature $kT = 1.9^{+0.3}_{-0.2}$ keV, an unabsorbed energy flux Φ(2-10 keV)= $5.7^{+1.3}_{-2.2} \times 10^{-13}$ erg cm^{-2} s^{-1}, and a p-value of 0.73. Given the low level of statistics, no spectral model can be rejected, as shown by the p-values. However, the fitted temperature of the black-body model is much higher than usually observed for cooling neutron stars (∼ 0.2 keV) or central compact objects (CCOs; ∼ 0.5 keV). Such a high temperature can be observed in bursting binary systems, but due to the lack of evidence of bursting behavior in X-rays, this scenario is not considered in the following discussion. Hence, the power-law model is adopted to characterise the X-ray emission of XMMU J183245−0921539 and it is displayed on Fig. 2.

[2] The p-value corresponds to the null-hypothesis probability

Because of the low statistics and the fact that the *XMM-Newton* observation was performed in imaging mode (timing resolutions of 2.6 s and 73 ms for MOS and pn instruments), no detailed pulsation search could be carried out. Future deeper observations in timing mode could provide better constraints on the nature of this X-ray source.

A comparison of the absorption along the line of sight obtained from the X-ray spectral model with the column depth derived from the atomic (HI) and molecular (^{12}CO, J=1→0 transition line) gas can be used to provide a lower limit on the distance to XMMU J183245−0921539, as described in Abramowski et al. (2011b). A minimal distance of ∼5 kpc is thus derived using the lower bound of the fitted N_H obtained with the power-law model.

3 A HADRONIC ORIGIN?

The Galactic Ring Survey (GRS) performed with the Boston University FCRAO telescopes (Jackson et al. 2006) provides measurements of the ^{13}CO (J=1→0) transition line covering the velocity range from -5 to 135 km s^{-1} in this region. The detection of this line is evidence for the presence of dense molecular clouds (MCs) that are known to be targets for cosmic-rays and hence gamma-ray emitters via neutral pion production and decay. Several MCs measured at different radial velocities are found around the source HESS J1832−093. The molecular structure showing the best spatial coincidence with the TeV emission is selected and shown in Fig. 4. The MC near distance of about 2.3 kpc given by the Galactic rotation curve model provided by Hou et al. (2009) is compatible with the distance estimate to the remnant. Following the approach described in Simon et al. (2001), the integrated antenna temperature on the MC velocity range is used to derive the gas mass of the structure which is ∼ 700 $M_\odot$, corresponding to a gas density of ∼ 20 cm^{-3}.

TeV emission from the direction of G22.7−0.2 might be related to protons either coming from the cosmic-ray (CR) sea or accelerated in early phases of a nearby SNR and interacting in dense molecular structures, producing neutral pions that decay into gamma rays. This scenario has already been invoked e.g. to explain "dark" TeV sources (e.g. Gabici et al. (2009)). For this hypothesis to work, localised high density target material is needed in order to explain that only a very small fraction of G22.7−0.2 emits gamma-rays. ^{13}CO measurements show the presence of such structures near HESS J1832−093, as seen on Fig. 4. Although no significant extension of the TeV source is detected, the upper limit of 0.074° is consistent with a slightly extended emission region as may be expected from the MC spatially coincident with HESS J1832−093. The expected bremsstrahlung emission from accelerated electrons can be neglected compared to the hadronic contribution since the proton to electron ratio p/e should be ≫ 100 for multi-TeV energies (e.g. Yuan et al. (2012) and references therein).

Using the mass and distance of the selected MC and following Eq. 10 of Aharonian (1991), the CR density enhancement factor k_{CR} can be estimated in units of the local CR density, corresponding to a value of 780. Such a high enhancement factor require the presence of a nearby CR source such as SNR G22.7−0.2 in order to explain the observed TeV emission. Moreover, Aharonian & Atoyan (1996) show that, given the SNR radius of about 10 pc and an assumed age around 10^3 yr, such a high k_{CR} value is expected for a slow diffusion coefficient of $D \sim 10^{27}$ cm^2 s^{-1} for 10 TeV hadrons, but excluded for a diffusion coefficient of $D \sim 10^{29}$ cm^2 s^{-1}. Therefore the hadronic origin of the VHE emission is possible in the case

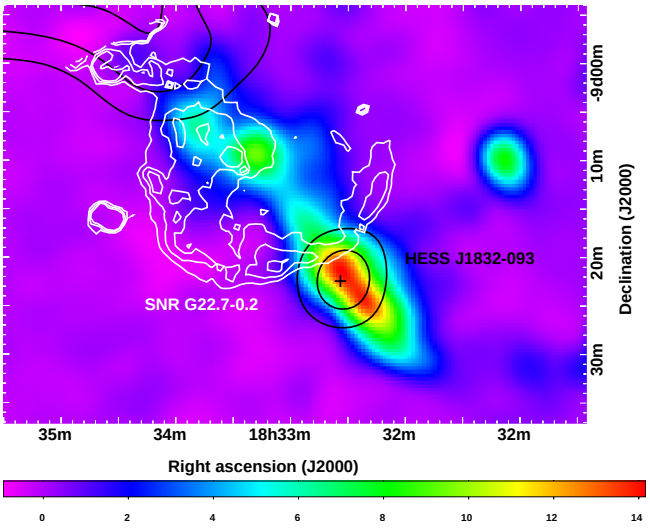


Figure 4. Integrated ^{13}CO antenna temperature in arbitrary units (Jackson et al. 2006) in a velocity range of 26 to 31 km s^{-1} smoothed with the average H.E.S.S. PSF for this data set. The gamma-ray excess of Fig. 1 is shown in black contours (50, 75 and 100 gamma levels) while the radio observation of SNR G22.7−0.2 (Helfand et al. 2006) at 1.4 GHz is overlaid in white contours. (0.002 and 0.005 mJy/beam). The black cross represents the best-fit position of the H.E.S.S. excess with corresponding errors.

of slow diffusion only. Similar diffusion coefficients are also needed in other studies such as for the VHE emission in spatial coincidence with dense MCs around SNR W28 (Aharonian et al. 2008).

4 A COMPACT NATURE

4.1 A faint PWN?

A likely scenario would be that both the X-ray and TeV sources stem from a PWN powered by a yet unknown pulsar. Even if the non-thermal aspect of the X-ray emission is not well determined, its hard spectral index for the PL assumption is indicative of an emission from the vicinity of a pulsar, e.g. magnetospheric or striped wind (e.g. Pétri & Lyubarsky 2007). Therefore, despite the lack of observed pulsations in the object, a pulsar origin for XMMU J183245−0921539 will be considered here. The TeV emission would then be attributed to inverse Compton emission coming from the nebula powered by the putative pulsar.

It can be tested whether energetically a PWN scenario plausibly matches with the population of known TeV-emitting PWNe, under the hypothesis that the X-ray emission comes from the pulsar's magnetosphere. The luminosity $L_{\rm X}(2-10\,{\rm keV})$ of the X-ray point source can be translated to an estimate of the $\dot{\rm E}$ of the hypothetical pulsar using the $L_{\rm X}/\dot{E}$ relation provided by Li et al. (2008). The estimated spin-down luminosity is of the order of 10^{37} erg s^{-1} for a distance of 5 kpc, pointing towards a rather young pulsar age ($\lesssim 10^5$ years). Note that the compact size of the TeV source is also an indication for a fairly young object. The $\dot{\rm E}/{\rm d}^2$ for the same distance is 6×10^{35}erg s^{-1}kpc^{-2}, corresponding to the band for which more than 40% of the PWNe are detected with H.E.S.S. (Klepser et al. 2013). Therefore, if the putative pulsar powers a TeV PWN, the latter should be detectable with the H.E.S.S. array. A very similar conclusion is derived if the detected X-ray emission is assumed to stem from the hard core of the X-ray PWN. The lack of an extended X-ray PWN around XMMU J183245−0921539 could be attributed to yet insufficient statistics and *XMM-Newton* angular resolution, or to the high absorption which would prevent any detection of the extension below 3 keV (due to synchrotron cooling of the electrons, the outer region of the PWN would have a softer index than its core). Another possibility would be that the X-ray PWN is underluminous (Kargaltsev et al. 2008). Future high-resolution X-ray observations are thus needed to clarify this issue. Together with the absence of detected X-ray pulsations, the PWN scenario is possible but remains for the moment still unconfirmed.

4.2 A new binary system?

The 2MASS catalog[3] lists three infrared sources around the position of XMMU J183245−0921539 within the *XMM-Newton* PSF of about 6″ (FWHM). However only one faint source is located within the statistic positional error (2.3″) of XMMU J183245−0921539. This source, 2MASS J18324516−0921545, lies 1.9″ away from the position of the X-ray source. No optical counterpart is found, likely due to strong extinction in the Galactic plane. The apparent magnitudes observed in the J, H, K bands are $m_J = 15.52 \pm 0.06$ mag, $m_H = 13.26 \pm 0.04$ mag, and $m_K = 12.17 \pm 0.02$ mag, respectively (Skrutskie et al. 2006). The probability of a chance association between 2MASS J18324516−0921545 and XMMU J183245−0921539 is around 2%, following the approach by Akujor (1987). To derive this value, all sources of the 2MASS catalog with $m_K \leqslant 13$ in a 2° side box around XMMU J183245−0921539 were selected, and the chance probability was computed to detect one of them in a surface of 16.6 arcseconds^2 corresponding to the *XMM-Newton* localisation error area.

The infrared source 2MASS J18324516−0921545 discovered in spatial coincidence with XMMU J183245−0921539 could suggest that the X-ray source resides in a binary system around a massive star. Variable TeV emission from a number of gamma-ray binaries has already been detected (Aharonian et al. 2005b, 2006c; Albert et al. 2009; Aliu et al. 2014). The optical brightness derived for 2MASS J18324516−0921545 is compatible with an association in a binary system with XMMU J183245−0921539 if the measured X-ray absorption is mainly stemming from local gas around the X-ray source. In the absence of orbitally modulated X-ray or TeV emission, the binary possibility remains unconfirmed, although the low chance probability association between the IR and X-ray sources seems to support this scenario. The non-detection of variability could be either due to insufficient statistics or due to a specific geometrical shape of the binary system that would not produce modulated emission in gamma-rays. Although one could expect strong GeV emission from gamma-ray binary systems, one of these objects has currently no GeV counterpart : HESS J0632+057. Therefore the non-detection in GeV of HESS J1832−093 does not rule out the binary scenario. Moreover, HESS J0632+057 was unidentified at the time of its discovery (Aharonian et al. 2007) and its variability was only confirmed later on (Hinton et al. 2009; Bongiorno et al. 2011). The similarities with HESS J0632+057 make HESS J1832−093 a very good binary system candidate despite the absence of modulated emission.

[3] http://www.ipac.caltech.edu/2mass/releases/allsky/

5 CONCLUSION

Observations in the field of view of SNR G22.7−0.2 have led to the discovery of the point-like source HESS J1832−093 lying on the edge of the SNR radio rim. Hadronic particles accelerated in the SNR G22.7−0.2 interacting with dense gas material could result in TeV emission through neutral pion production and decay in the case of slow CR diffusion.

On the other hand, a compelling X-ray counterpart, XMMU J183245−0921539, has been discovered, whose nature is yet to be established. Together with the TeV emission and the infrared point source 2MASS J18324516−0921545, plausible object classifications are a young pulsar wind nebula or a gamma-ray binary. Following the case of HESS J1943+213, an extragalactic origin such as an AGN could also be possible. However this scenario was disfavored due to the lack of GeV emission and point-like counterparts in radio data.

The TeV source properties strongly resemble the situation of HESS J0632+057 at the time of its discovery (Aharonian et al. 2007), which only after extensive continued monitoring in X-rays and gamma-rays could be identified as a gamma-ray binary (Hinton et al. 2009; Acciari et al. 2009; Bongiorno et al. 2011). Point-like sources remain rare amongst all newly discovered VHE sources and HESS J1832−093 is an excellent candidate for belonging to the rare and special class of gamma-ray binaries.

Nevertheless, given the lack of a clear confirmation of the binary scenario through variability, other scenarios are also possible. The isolated PWN scenario, however, lacks an X-ray PWN detection despite XMM-Newton coverage, and the cosmic-ray-molecular cloud interaction scenario is hard to reconcile with the possible association of XMMU J183245−0921539 with HESS J1832−093. Further multiwavelength studies are therefore encouraged to establish (or ultimately reject) HESS J1832−093's classification as illuminated molecular cloud, gamma-ray binary or pulsar wind nebula.

ACKNOWLEDGEMENTS

The support of the Namibian authorities and of the University of Namibia in facilitating the construction and operation of H.E.S.S. is gratefully acknowledged, as is the support by the German Ministry for Education and Research (BMBF), the Max Planck Society, the French Ministry for Research, the CNRS-IN2P3 and the Astroparticle Interdisciplinary Programme of the CNRS, the U.K. Science and Technology Facilities Council (STFC), the IPNP of the Charles University, the Czech Science Foundation, the Polish Ministry of Science and Higher Education, the South African Department of Science and Technology and National Research Foundation, and by the University of Namibia. We appreciate the excellent work of the technical support staff in Berlin, Durham, Hamburg, Heidelberg, Palaiseau, Paris, Saclay, and in Namibia in the construction and operation of the equipment.

This publication makes use of molecular line data from the Boston University-FCRAO Galactic Ring Survey (GRS). The GRS is a joint project of Boston University and Five College Radio Astronomy Observatory, funded by the National Science Foundation under grants AST-9800334, AST-0098562, & AST-0100793

This publication makes use of data products from the Two Micron All Sky Survey, which is a joint project of the University of Massachusetts and the Infrared Processing and Analysis Center/California Institute of Technology, funded by the National Aeronautics and Space Administration and the National Science Foundation.

REFERENCES

Abramowski A. et al., 2011a, A&A, 529, A49
Abramowski A. et al., 2011b, A&A, 531, A81
Acciari V. A. et al., 2009, ApJ, 698, L94
Ackermann M. et al., 2012, ApJS, 203, 4
Aharonian F. et al., 2005a, A&A, 432, L25
Aharonian F. et al., 2005b, A&A, 442, 1
Aharonian F. et al., 2008, A&A, 481, 401
Aharonian F. et al., 2006a, A&A, 457, 899
Aharonian F. et al., 2006b, ApJ, 636, 777
Aharonian F. et al., 2006c, A&A, 460, 743
Aharonian F. A., 1991, Ap&SS, 180, 305
Aharonian F. A. et al., 2007, A&A, 469, L1
Aharonian F. A., Atoyan A. M., 1996, A&A, 309, 917
Akujor C. E., 1987, Astrophysics and Space Science, 135, 187
Albert J. et al., 2009, ApJ, 693, 303
Alexander T., 1997, in Astrophysics and Space Science Library, Vol. 218, Astronomical Time Series, Maoz D., Sternberg A., Leibowitz E. M., eds., p. 163
Aliu E. et al., 2014, ApJ, 780, 168
Atwood W. B. et al., 2009, ApJ, 697, 1071
Becherini Y., Djannati-Ataï A., Marandon V., Punch M., Pita S., 2011, Astroparticle Physics, 34, 858
Bongiorno S. D., Falcone A. D., Stroh M., Holder J., Skilton J. L., Hinton J. A., Gehrels N., Grube J., 2011, ApJ, 737, L11
Carter J. A., Read A. M., 2007, A&A, 464, 1155
Gabici S., Aharonian F. A., Casanova S., 2009, MNRAS, 396, 1629
Guseinov O. H., Ankay A., Sezer A., Tagieva S. O., 2003a, Astronomical and Astrophysical Transactions, 22, 273
Guseinov O. H., Ankay A., Tagieva S. O., 2003b, Serbian Astronomical Journal, 167, 93
Helfand D. J., Becker R. H., White R. L., Fallon A., Tuttle S., 2006, AJ, 131, 2525
Hinton J. A. et al., 2009, ApJ, 690, L101
Hou L. G., Han J. L., Shi W. B., 2009, A&A, 499, 473
Jackson J. M. et al., 2006, ApJS, 163, 145
Kargaltsev O., Pavlov G. G., Wong J. A., 2008, ArXiv e-prints, 0805.1041
Klepser S. et al., 2013, ArXiv e-prints
Li X.-H., Lu F.-J., Li Z., 2008, ApJ, 682, 1166
Nolan P. L. et al., 2012, ApJS, 199, 31
Pétri J., Lyubarsky Y., 2007, A&A, 473, 683
Shaver P. A., Goss W. M., 1970, Australian Journal of Physics Astrophysical Supplement, 14, 133
Simon R., Jackson J. M., Clemens D. P., Bania T. M., Heyer M. H., 2001, ApJ, 551, 747
Skrutskie M. F. et al., 2006, AJ, 131, 1163
Yuan Q., Liu S., Bi X., 2012, ApJ, 761, 133